Journal of
Nanoscience and Nanotechnology
Vol. 11, 5698–5701, 2011

RESEARCH ARTICLE

Charging Effect in Au Nanoparticle Memory Device with Biomolecule Binding Mechanism

Sung Mok Jung[1], Hyung-Jun Kim[1], Bong-Jin Kim[1], Tae-Sik Yoon[2], Yong-Sang Kim[2], and Hyun Ho Lee[1,*]

[1] *Department of Chemical Enginnering, Myungji University, Gyeonggi Yongin 449-728, Korea*
[2] *Department of Nano Enginnering, Myungji University, Gyeonggi Yongin 449-728, Korea*

Organic memory device having gold nanoparticle (Au NPs) has been introduced in the structure of metal-pentacene-insulator-silicon (MPIS) capacitor device, where the Au NPs layer was formed by a new bonding method. Biomolecule binding mechanism between streptavidin and biotin was used as a strong binding method for the formation of monolayered Au NPs on polymeric dielectric of poly vinyl alcohol (PVA). The self-assembled Au NPs was functioned to show storages of charge in the MPIS device. The binding by streptavidin and biotin was confirmed by AFM and UV-VIS. The UV-VIS absorption of the Au NPs was varied at 515 nm and 525 nm depending on the coating of streptavidin. The AFM image showed no formation of multi-stacked layers of the streptavidin-capped Au NPs on biotin-NHS layer. Capacitance–voltage (*C–V*) performance of the memory device was measured to investigate the charging effect from Au NPs. In addition, charge retention by the Au NPs storage was tested to show 10,000 s in the *C–V* curve.

Keywords: Au NPs, PVA, *C–V*, Hysteresis.

1. INTRODUCTION

During the past years, organic memory devices using nanoparticles (NPs) as floating gate (FG) have been studied intensively.[1–4] Before the introduction of the organic memory device, nonvolatile memory systems have been typically studied on Si, Ge, $NiSi_2$, Pt, and Au nanocrystals (NCs) serving as the charge storage elements.[1,5–7] They have been shown to exhibit excellent memory performance and potential scalability. At present, conventional flash memory cell is fabricated based on nanoscale metal oxide field effect transistor (MOSFET).[5,6] Thus, the manufacturing processes are highly costy and complicated. However, recent demand for flexible electronic applications necessitates the organic electronic structure. Flexibility is particularly important for the future applications such as foldable and wearable electronics. So far, organic semiconductor such as pentacene has been widely used for the semiconductor material in the field of organic electronics. However, due to the low mobility of pentacene-based device, the electrical performance of pentacene is far behind of the silicon-based electronic device for high speed operational device.[2,3] Therefore, it can be suggested that the organic device for flexible electronics may have other breakthrough than the high speed device in electronic application, such as memory device. Organic flexible memories may have merits of simple fabrication steps, low temperature in fabrication, and low cost in manufacturing process. For organic based memory device, unlike poly-silicon as floating gate in conventional flash memory, charges are stored in discontinuous NPs instead of a continuous charging layer of poly-silicon. Therefore, there are some risks that stored charges in isolated NPs cannot easily redistribute amongst themselves.[6,7]

The biomolecules are often used in the fabrication of the memory device.[7–9] Cage-shaped supramolecular protein array was used for the matrix of nano-sized pattern with bio nanodot (BND)[7] or viruses containing metal nanoparticles were used for the charging elements.[8] In this paper, polymeric PVA was adopted as dielectric layer in MPIS capacitor for Au NPs charging layer, which was intervened by biomolecule binding mechanism.[9] The binding of streptavidin and biotin has been widely used to have a strong binding of NPs to surface.[10,11] The Au NPs were coated by streptavidin and monolayered on biotin-coated PVA layer.

*Author to whom correspondence should be addressed.

 1533-4880/2011/11/5698/004 doi:10.1166/jnn.2011.4376

The charging effect by Au NPs was confirmed and investigated in details in terms of C–V hysteresis. The streptavidin-coated Au NPs was confirmed by UV-VIS measurement and FTIR. Without the Au NPs layer, PVA based capacitor does not show any noticeable C–V hysteresis on small voltage sweep of (+/−)2 V to (+/−)4 V.

2. EXPERIMENTAL DETAILS

To prepare polymeric dielectric layer, 5.0 wt% of PVA (Kanto Chemical Co., Japan) in DI water was mixed for 3 hrs and ADC (ammonium dichromate, Kanto Chemical Co., Japan) was added to the solution as a cross-linking agent. The PVA solution was spin-coated on p-type Si wafer as a gate insulator. Then, it was crosslinked by UV exposure with thickness of 250 nm. APTES (3-Aminopropyl-triethoxysilane, 99%, Aldrich) was deposited by dip-coating at 5% wt. solution with ethanol in order to immobilize amine group on PVA surface. 50 μm/ml of Biotin-NHS (3-sulfo-N-hydroxy-succinimide ester sodium salt, Sigma-Aldrich) was dissolved in DI water. APTES coating layer on PVA surface was then immersed in the biotin solution for fixing biotin or biotinylation on the APTES. Au NPs of 5 nm diameter was purchased by British Bio Cell International (#EM.GC5/4, 5×10^{13} particles/ml). The Au NPs were capped by streptavidin for one hour, which was diluted in DI water. Au NPs after capping was recovered by centrifugation with a microcentrifuge tube with filtering function. Uncapped streptavidin was washed out by the filtration. Then, the device coated by biotin molecule was dip-coated in streptavidin-capped Au NPs solution for 30 mins, respectively. For removing unbound Au NPs, the device was rinsed in DI water for 3 mins.[9] Pentacene active layer and gold electrode (0.5 mm diameter) were deposited by thermal evaporator with 60 nm and 200 nm of thickness, respectively. Figure 1 shows a schematic structure of nonvolitle memory device with polymeric dielectric layer. C–V performance was measured by HP Agilent 4284 A at 1 MHz of frequency. Conjugation of streptavidin on the Au NPs was confirmed by UV-VIS (UV-1601, Shimazu, Japan).

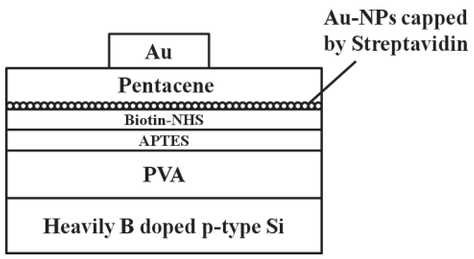

Fig. 1. Schematic diagram of non-volatile organic MPIS memory device.

3. RESULTS AND DISCUSSION

Figure 2 shows UV-VIS spectra of intrinsic Au NPs and Au NPs coated with streptavidin. The conjugation of streptavidin on the surface of Au NPs was easily accomplished by one hour incubation.[10] The intrinsic Au NPs were detected at 515 nm wavelength for Au NPs with 5 nm diameter. Difference of detectable wavelength of Au NPs coated with streptavidin was significantly observed in Figure 2. While the Au NPs without any capping or coating was confirmed at 515 nm, the detectable wavelength of Au NPs coated with streptavidin was 525 nm. It was reported that 40 nm Au NPs showed 5 nm longer absorption in UV-VIS spectra with the streptavidin conjugation.[10] It can be explained that shift of detection peak from 515 nm to 525 nm in Figure 2 was caused by capping with streptavidin.[9, 10] Therefore, the UV-VIS spectra in Figure 2 confirmed the successful conjugation of the streptavidin on the Au NPs.

In the fabrication process of the biotin-coated surface, the amine groups in APTES were functionalized on the PVA surface. Then, the biotin-NHS was dip-coated on the APTES treated surface (biotinylation process). The amine group of the APTES and the subsequently processed biotinylated surface were confirmed by FTIR(data not shown).[9] The biotinylated surface was immediately dip-coated with the streptavidin-conjugated Au NPs before the contamination of the biotin in an ambient environment.

Figure 3 shows AFM image of the self-assembled monolayer of Au NPs on biotin functionalized PVA surface. The AFM result in Figure 3 shows an uneven layer of Au NPs on the APTES-coated surface was formed. In AFM image of Figure 3, individual Au nanoparticle could not be clearly imaged. Instead, there are some Au NPs that are aggregated. However, their surface roughness showed that no multi-stacked Au NPs existed, which indicates that

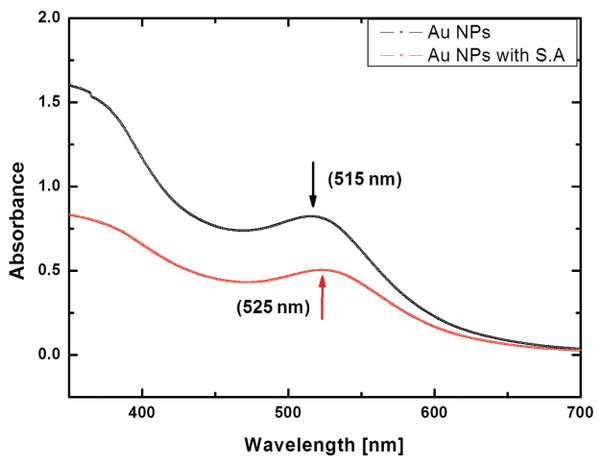

Fig. 2. UV-VIS spectra of intrinsic Au NPs and Au NPs coated with streptavidin.

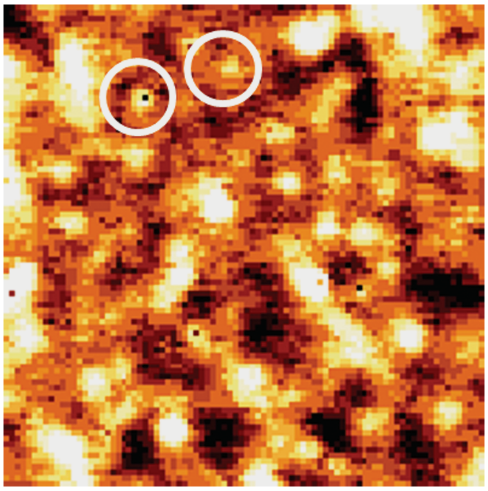

Fig. 3. AFM image of Au nanoparticles on the biotinylated surface of PVA.

the aggregates were two-dimensional. The rms of surface roughness was measured as 2.76 nm. The empty regions formed by the agglomerated particles will be a source of defects in its capacitor device.

Figure 4 shows the *C–V* results of metal-insulator-silicon (MIS) structure capacitor device without any NPs intervening layer. In Figure 4, the *C–V* curve of MIS capacitor shows the conventional electric characteristics of capacitor using *p*-type Si substrate. Flatband voltage (V_{FB}) was changed depending on voltage sweeping (+/−)2 V or (+/−)3 V due to the effect of mobile ion in PVA gate insulator. In Figure 4, the *C–V* curves has no hysteresis loops between forward direction sweep and backward direction sweep for both (+/−)2 V or (+/−)3 V sweeping ranges. However, in a separate measurement, increase of voltage sweep range, for example, (+/−)7 V or higher voltage range, resulted in hysteresis loop without charging layer with PVA dielectric (data not shown). For the hysteresis in the high voltage sweep with PVA film, electron injection from the top electrode and charge trapping inside of the PVA layer is driving the hysteresis behavior under negative gate bias. In addition, the other reason of *C–V* hysteresis will be mobile ions. The cross-linked PVA layer has ions like Cr^{2-} (negative mobile ions) from ammonium dichromate for the complex formation.[12] When the device is applied with a negative bias, the ions are forced to move near silicon substrate, resulting in the VFB shift to right direction. In contrast, when the device is applied with a positive bias, the ions can move to near gate. However, in this study, these hysteresis effects could not be apparently observed with low range of voltage sweep, such as (+/−)2∼4 V.

Figure 5 shows the *C–V* results of MPIS nonvolatile memory device under 1 MHz of frequency. For the *C–V* measurement, voltage sweeping range was varied from (+/−)2 V to (+/−)4 V. For all voltage sweep ranges, sustainable hysteresis behaviors were detected, which are particularly from the charging effect in the Au NPs. Since the PVA dielectric (250 nm) is thick enough not to have a significant leakage, all hysteresis loops have clockwise directions. It indicates that hole injection into pentacene layer from top electrode and charging in Au NPs is the major mechanism for the charging effect. In addition, compared with *C–V* behaviors measured with 10 nm SiO_2 dielectric, the capacitance itself with PVA dielectric is lower than that with the SiO_2 due to the thick layer of the PVA.[9]

Voltage sweep for the device from accumulation to inversion was set with 0.1 V step level. In Figure 5, sweep voltage from −2 V to +2 V made V_{FB} at positive voltage region. In inversion region, however, the V_{FB} was shifted to negative voltage region due to the charge trapping by Au NPs. The ΔV_{FB} was measured as 1.2 V for the (+/−)2 V sweeping. The memory window of ΔV_{FB} in the (+/−)3 V range was 1.9 V and 2.6 V of memory window was measured for the (+/−)4 V sweep. Therefore, the increase of voltage sweeping range makes more

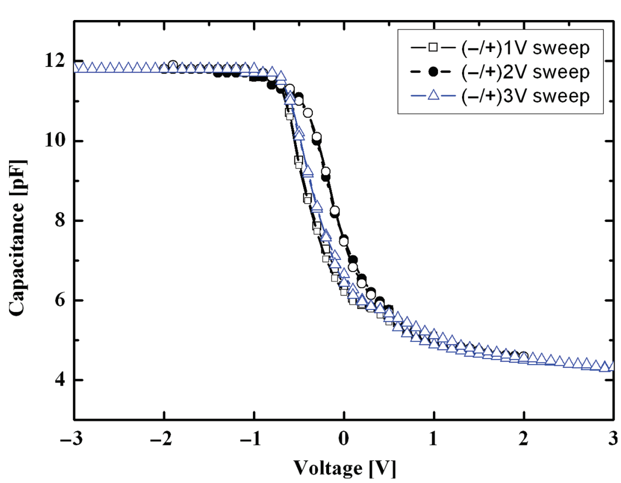

Fig. 4. *C–V* results of MIS device structure using organic PVA insulator under 1 Mhz frequency.

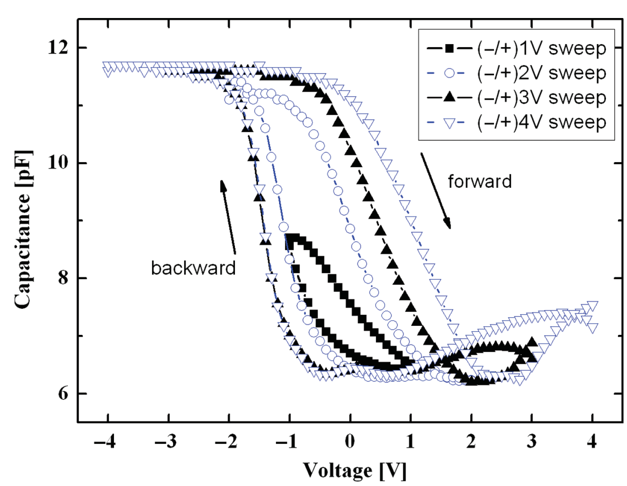

Fig. 5. *C–V* results of non-volatile organic memory device with range of 1, 2, 3 and 4 V under 1 Mhz frequency.

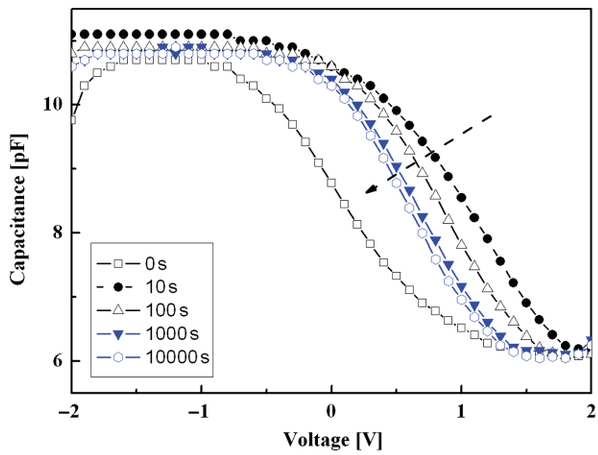

Fig. 6. Retention characteristics of the non-volatile memory structure with Au NPs using a −7 V electrode voltage stress for 10 s at room temperature.

charging effects to Au-NPs. The hysteresis behaviors by increasing sweep voltage range of (+/−)2 V, (+/−)3 V and (+/−)4 V show the difference at accumulation region. From (+/−)2 V range to (+/−)3 V range, V_{FB} at both directions were shifted to negative voltage and positive voltage, respectively. However, in (+/−)4 V sweep, only V_{FB} at inversion region was shifted to positive voltage. It indicates that the hole trapping through the top electrode is limited over 3 V, while the electron trapping through the top electrode is allowed over 3 V. However, more detailed studies are required for the mechanism.

Retention characteristic of the MPIS memory device on *C–V* results is shown in Figure 6. Bias voltage of −7 V was applied for 10 s at room temperature to top electrode in order to inject electrons to Au NPs. On measurements of *C–V* between the 10 s and 100 s after the bias, the electron charges stored were significantly reduced. It means that electrons trapped by the Au NPs were unstable and easily extractable to electrode. As shown in Figure 6, after the electrons stored at Au NPs were extracted largely for 100 s and 1,000 s, the reduction rate of storing charges went down. Therefore, there was no big difference between the *C–V* curve of 1,000 s and 10,000 s.

4. CONCLUSIONS

Nonvolatile organic memory device with PVA gate insulator having self assembled Au NPs by protein binding was fabricated and characterized. The *C–V* characteristics of the device showed hysteresis loop caused by charge injection to Au NPs from top electrode. The capping of Au NPs with streptavidin was confirmed by UV-VIS. The retention for charge storage by the Au NPs was also characterized. The device can be further developed to a sensing device which can detect specific biomolecules using antigen-antibody binding.

Acknowledgments: This work is financially supported by the Ministry of Knowledge Economy (MKE) of Korean Government and Korea Institute for Advancement in Technology (KIAT) through the Workforce Development Program in Strategic Technology.

References and Notes

1. W. L. Leong, P. S. Lee, S. G. Mhaisalkar, T. P. Chen, and A. Dodabalapur, *Appl. Phys. Lett.* 90, 042906 (**2007**).
2. S. Paul, C. Pearson, A. Molloy, M. A. Cousins, M. Green, S. Kolliopoulou, P. Dimitrakis, P. Normand, D. Tsoukalas, and M. C. Petty, *Nano Lett.* 4, 533 (**2003**).
3. M. F. Mabrook, C. Pearson, D. Kolb, D. A. Zeze, and M. C. Petty, *Organ. Electron.* 9, 816 (**2008**).
4. M. F. Mabrook, A. S. Jombert, S. E. Machin, C. Pearson, D. Kolb, K. S. Coleman, D. A. Zeze, and M. C. Petty, *Mater. Sci. Eng. B* 159, 14 (**2009**).
5. P. H. Yeh, L. J. Chen, P. T. Liu, D. Y. Wang, and T. C. Chang, *J. Nanosci. Nanotechnol.* 7, 339 (**2007**).
6. P. H. Yeh, L. J. Chen, P. T. Liu, D. Y. Wang, and T. C. Chang, *Electrochim. Acta.* 52, 2920 (**2007**).
7. A. Miura, R. Tsukamoto, S. Yoshi, I. Yamashita, Y. Uraoka, and T. Fuyuki, *Nanotechnol.* 19, 255201 (**2008**).
8. N. G. Portney, A. A. Martinez-Morales, and M. Ozkan, *ACS Nano* 2, 191 (**2008**).
9. S. M. Jung, H.-J. Kim, B.-J. Kim, T.-S. Yoon, Y.-S. Kim, and H. H. Lee, *Appl. Phys. Lett.* 97, 153302 (**2010**).
10. H. K. Park, Y. T. Lim, J. K. Kim, H. G. Park, and B. H. Chung, *Ultramicro.* 108, 1115 (**2008**).
11. W.-D. Moll and P. Guo, *J. Nanosci. Nanotechnol.* 7, 1 (**2007**).
12. L. Grimm, K.-J. Hilke, and E. Scharrer, *J. Electrochem. Soc.* 130, 1767 (**1983**).

Received: 2 August 2010. Accepted: 15 January 2011.